Molybdenum binding to soil constituents in acid soils: an XAS and modelling study

Jon Petter Gustafsson[a,b,*] and Charlotta Tiberg[a]

[a]*Department of Soil and Environment, Swedish University of Agricultural Sciences, Box 7014, 750 07 Uppsala, Sweden*

[b]*Division of Land and Water Resources Engineering, KTH Royal Institute of Technology, Brinellvägen 28, 100 44 Stockholm, Sweden*

*Corresponding author. E-mail address: jon-petter.gustafsson@slu.se

Highlights:

- Molybdenum(VI) is bound to ferrihydrite and aluminium hydroxide predominantly as tetrahedral, edge-sharing inner-sphere and outer-sphere complexes.
- On natural organic matter, molybdenum(VI) is bound at low pH as an octahedrally coordinated monomeric complex.
- Results for a spodic B horizon show an $Al(OH)_3$-type phase to be an important sorbent for molybdenum(VI).
- The results were used to suggest new complexation constants for the CD-MUSIC and Stockholm Humic models.

Abstract

Despite its importance as a trace element, the binding mechanisms of molybdenum in soils are not well known. In this study, we studied the binding of molybdenum onto selected soil samples, and we used X-ray absorption spectroscopy (XAS) to characterise the coordination of molybdenum on three important environmental sorbents: ferrihydrite (Fh), amorphous aluminium hydroxide ($Al(OH)_3$) and fulvic acid. The X-ray near-edge structure (XANES) data showed that the added molybdenum(VI) was not reduced, although for the organic samples the coordination shifted from tetrahedral to octahedral. The EXAFS (extended X-ray absorption fine structure) analysis showed that molybdenum(VI) on Fh and $Al(OH)_3$ was dominated by edge-sharing bidentate complexes with Mo···Fe and Mo···Al distances of 2.80 and 2.62 Å, respectively. For ferrihydrite, there was a minor contribution from a corner-sharing bidentate complex at 3.55 Å. Further, geochemical modelling suggested an additional role of an outer-sphere complex at high pH. A sample from a spodic Bs horizon had XANES and EXAFS features similar to those of Mo sorbed to $Al(OH)_3$, highlighting the importance of $Al(OH)_3$-type sorbents in this soil. However, in the studied organic samples molybdenum(VI) was present in a distorted octahedral configuration as an organic complex. The results were used to improve molybdenum binding reaction equilibrium constants in the CD-MUSIC model for ferrihydrite and in the Stockholm Humic Model. Collectively the results show that acid soils may contain sorbents able to bind molybdenum efficiently, and thus prevent its leaching to waters.

1. Introduction

Molybdenum (Mo) is an essential trace element with an important role in the biogeochemical cycle of nitrogen (N), as it is required for N fixation and denitrification. The Mo-containing enzyme nitrogenase catalyzes the reaction. In the most common form of this enzyme, molybdenum and iron are co-factors, where molybdenum is coordinated to a sum of about six oxygen and sulphur atoms in a distorted octahedral configuration (Burgess, 1990). Molybdenum deficiency in soils has frequently been reported, especially under P-deficient conditions (Murphy and Walsh, 1972; Wurzberger et al. 2012). However, molybdenum is also a potentially toxic contaminant that may be released from e.g. municipal solid waste incinerator bottom ash (Meima et al. 2002). The toxicity of molybdenum is related primarily to its interaction with copper and sulphur, causing copper deficiency in ruminants (Suttle, 1991).

Under conditions typical for most aerated soils, dissolved molybdenum exists primarily as dissolved molybdate (MoO_4^{2-}) ions. Adsorption to hydrous oxides is thought to be an important mechanism that restricts the mobility of molybdenum in the environment. For a long time it has been known that molybdate is bound to a variety of different iron(III) and aluminium(III) (hydr)oxides (Jones, 1957; Reisenauer et al. 1962). Examples include ferrihydrite (Gustafsson, 2003; Kashiwabara et al. 2011), goethite (Bibak and Borggaard, 1994; Arai, 2010), hematite (Goldberg et al. 1996), gibbsite (Manning and Goldberg, 1996; Miedaner et al. 2011) and alumina (Spanos et al. 1990). In addition, molybdate is bound also to titanium oxides such as titania (Bourikas et al. 2001). Molybdate adsorption is strongly pH-dependent with strong adsorption at low pH (below about 6) to weak or insignificant adsorption at higher pH. Further, competition with other anions modifies the extent of molybdate adsorption. For example, phosphate competes strongly for available adsorption sites, particularly at high pH (Gustafsson, 2003; Xu et al. 2006a). So far, relatively few

studies have reported the coordination mode of adsorbed molybdate on (hydr)oxides. Goldberg et al. (2008) used attenuated total reflectance infrared (ATR-FTIR) and Raman spectroscopy and concluded that molybdate formed an inner-sphere surface complex on amorphous aluminum oxide at low pH, which shifted to an outer-sphere surface complex at high pH. Arai (2010), who studied molybdate adsorption on goethite, used extended X-ray absorption fine structure (EXAFS) spectroscopy at the Mo K edge and obtained evidence for both corner-sharing and edge-sharing bidentate complexes involving the tetrahedral molybdate anion. In addition, he observed octahedrally coordinated MoO_6 polymers at low pH. In another Mo K-edge EXAFS study, molybdate adsorption on ferrihydrite was found to involve mostly outer-sphere complex formation, as there was only a minor contribution from second-shell Fe (Kashiwabara et al. 2011); however, it should be noted that the pH value was high (8), which may be important when interpreting these results.

Molybdenum(VI) may also be bound to natural organic matter (NOM). Already in 1967, sorption of molybdate to humic acid was observed (Szilagyi, 1967). Consistent with this, Bibak and Borggaard (1994) observed significant molybdate adsorption to organic matter especially at low pH (< 5). Wichard et al. (2009) added molybdate to leaf litter and soil samples. They used Mo K-edge EXAFS and XANES (X-ray absorption near edge structure) spectroscopy to identify the reaction products. Their interpretation was that molybdenum formed complexes with tannins and tannin-like compounds, as well as to iron oxides. Additional evidence for the importance of natural organic matter for molybdenum binding has recently been obtained using stable isotopes (Siebert et al. 2015)

Surface complexation models have frequently been used to describe molybdate adsorption to hydrous oxides. Most previous attempts, however (e.g. the CD-MUSIC model of Gustafsson, 2003) did not constrain the model based on structural observations, and may therefore rely on incorrect assumptions as regards the coordination environment of the bound

molybdate. Goldberg et al. (2008) were the first (and until now the only) authors who attempted to design such a model based on spectroscopic observations (in their case vibrational spectroscopy); they used the triple layer model to optimize surface complexation constants and found that the model agreed well with data for iron(III)/aluminium (hydr)oxides and mineral soils. As concerns molybdenum complexation onto natural organic matter, no model currently exists.

The objective of this work was to obtain information on the coordination of adsorbed molybdate on selected sorbents, ferrihydrite, amorphous aluminium hydroxide, and natural organic matter, all of which are likely to be of importance for Mo binding in acid soils, and to investigate whether the coordination of molybdate added to two soil horizons from a Spodosol could be understood based on these observations. Moreover, we investigated whether it was possible to use the spectroscopic data to design complexation models that capture the binding of molybdate to ferrihydrite and to natural organic matter in acid soils.

2. Materials and methods

2.1 Soils

Soil samples were collected from 4 soils from different locations in central Sweden. Two of these were Albic Podzols (Risbergshöjden and Storå), one was a Eutric Arenosol (Björkby Sand), and one was a Fibric Histosol (Paskalampa), according to IUSS Working Group WRB (2014). From the Risbergshöjden and Storå soils, O as well as Bs horizons were sampled. Selected chemical properties are shown in Table 1. The soils were sieved immediately after collection.

For field-moist mineral soils a 4 mm sieve was used in accordance with standardized leaching test procedures (ISO TS 21268:2; ISO, 2008), while for organic soils an 8 mm sieve was used to facilitate the removal of coarse roots and branches. The soil samples were stored

in a field-moist state at +5°C for a maximum of three months before the experiments. The spodic B horizons (Risbergshöjden Bs2 and Storå Bs) were both characterized by low clay content (≤ 4%). Both had appreciable amounts of oxalate-extractable Si (Table 1) and an $(Al_{ox}-Al_{pyp})/Si_{ox}$ ratio of 2.0 and 2.2, respectively. These observations suggest that imogolite-type materials, mostly allophane, are the predominant secondary Al phases in these soils (Gustafsson et al. 1995; Gustafsson et al. 1999). Imogolite-type materials were also identified in the Risbergshöjden Bs horizon by Kleja et al. (2005).

Table 1

Properties of investigated soil samples

Soil	pH(H_2O)	Organic C	Clay	Fe_{ox}[a]	Al_{ox}[a]	Si_{ox}[a]	Al_{pyp}[b]
		%	%		mmol kg^{-1}		mmol kg^{-1}
Paskalampa Oi	3.8	46.7	< 1	39	16	0	14
Risbergshöjden Oe	3.8	47.9	< 1	13	30	0	22
Storå Oe	3.8	48.7	< 1	8	21	0.1	16
Björkby sand A	4.5	6.4	14	65	67	3	61
Risbergshöjden Bs2	5.7	0.8	4.0	74	519	233	43
Storå Bs	5.3	1.3	2.9	63	350	121	79

[a] Extracted with 0.2 M oxalate buffer at pH 3.0 (van Reeuwijk, 1995)

[b]Extracted with 0.1 M $Na_4P_2O_7$ (van Reeuwijk, 1995)

2.2. Model sorbents

2-line ferrihydrite (Fh) was prepared according to Swedlund and Webster (1999) and Schwertmann and Cornell (2000). A mixture of 36 mmol L^{-1} $Fe(NO_3)_3$ and 12 mmol L^{-1} $NaNO_3$ was brought to pH 8.0 through dropwise addition of 4 mol L^{-1} NaOH (prepared immediately before use). The resulting suspension was aged for 16 h at 20°C. Iron (hydr)oxide particles from such a suspension have been confirmed to be Fh using Fe K-edge

EXAFS spectroscopy (Gustafsson et al., 2007); moreover, use of X-ray diffraction confirmed the presence of Fh (data not shown). After synthesis the Fh suspension was back-titrated with 0.1 mol L^{-1} HNO_3 to pH 4.6 and stirred for about 30 min just before starting the batch experiments to avoid the presence of excessive CO_2 in the suspensions.

Amorphous aluminum hydroxide ($Al(OH)_3$) was prepared in a similar way as 2-line ferrihydrite, i.e. by mixing 36 mmol L^{-1} $Al(NO_3)_3$ and 12 mmol L^{-1} $NaNO_3$. The solution was then brought to pH 7.0 with 4 mol L^{-1} NaOH, and then the suspension was aged for 16 h. After synthesis, the $Al(OH)_3$ suspension was back-titrated to pH 5, and stirred for about 30 min before the batch experiments. X-ray diffraction confirmed that the formed $Al(OH)_3$ was amorphous in nature (data not shown).

2.3. Batch experiments

Briefly, either 1.00 g (for Risbergshöjden Oe and Storå Oe) or 2.00 g (other soils) field-moist soil was suspended in 30 mL solutions of variable composition in polypropylene centrifuge tubes, and then shaken for 7 days in a shaking water bath at 8^{o}C. This temperature was chosen for two reasons: (i) it represents the mean annual air temperature at the site, and (ii) it ensures that the microbial activity remains low during the equilibration period. The molybdenum(VI) binding following a Mo addition of 50 µmol L^{-1} Na_2MoO_4 was studied. This corresponds to molybdenum(VI) additions of 5.88, 5.88, 6.00, 0.83, 0.87, and 1.7 mmol Mo kg^{-1} dw for Risbergshöjden Oe, Storå Oe, Paskalampa Oi, Risbergshöjden Bs2, Björkby Sand A and Storå Bs, respectively. To produce a range of pH values in the suspensions, various amounts of acid (as HNO_3) or base (NaOH) were added, so that each system was studied at eight different pH values. For the organic soils (Risbergshöjden Oe, Paskalampa Oi and Storå Oe), the concentration of added Na_2MoO_4 was varied to investigate the influence on

the equilibrium molybdenum(VI) solution concentration on the amount adsorbed. All experiments were made using a background electrolyte of 0.01 mol L^{-1} $NaNO_3$. However, for Risbergshöjden Oe experiments were carried out also in 0.1 mol L^{-1} $NaNO_3$ to study the effect of ionic strength. To evaluate possible competition effects from phosphate on molybdenum(VI) adsorption to organic matter, an additional data set was produced for the Paskalampa Oi sample in which 50 µmol L^{-1} molybdenum(VI) was added together with 1.4 mmol L^{-1} NaH_2PO_4.

After equilibration, the suspensions were centrifuged at 5000*g* for 20 min, the pH values of the aqueous phases were measured (with a Radiometer glass combination electrode), and they were filtered (Acrodisc PF 0.2 µm) at the experimental temperature. Total dissolved concentrations of Mo and a number of other elements such as Ca, Mg, Al, and P were determined by plasma emission spectroscopy, with precautions to prevent Mo sorption to container walls (Gustafsson, 2003). Some reacted samples were then stored at +5^{o}C for analysis with XAS (X-ray absorption spectroscopy). The samples were stored for a maximum of one week before analysis.

We also conducted batch experiments with molybdenum(VI) in Fh and $Al(OH)_3$ suspensions to prepare samples for XAS analysis. In these experiments, 50 µmol L^{-1} molybdenum(VI) (as Na_2MoO_4) was equilibrated in suspensions of either Fh or $Al(OH)_3$ (1 mmol L^{-1} total Fe or 1 mmol L^{-1} total Al, respectively), in a background electrolyte of 0.01 mol L^{-1} $NaNO_3$. 200 µmol L^{-1} o-phosphate (as NaH_2PO_4) was also added to some suspensions to study the effect of competition. pH adjustments were made with either dilute NaOH or HNO_3 to obtain the desired pH values. The samples were shaken for 24 h and then processed as described above concerning filtration, centrifugation, pH measurement and molybdenum determination. The precipitated wet pastes of Fh or $Al(OH)_3$ were stored at +5^{o}C until XAS analysis three days later.

In a separate experiment, 2.8 mmol L^{-1} molybdenum(VI) was mixed with 7.8 g L^{-1} SRFA (Suwannee River Fulvic Acid, purchased from the IHSS, International Humic Substances Society) in a 0.01 mol L^{-1} $NaNO_3$ background. The pH was adjusted to 4.2 using 1 mol L^{-1} NaOH. The resulting solution was then left to stand and subjected to XAS analysis 10 hours later. Table 2 provides a summary of all samples used in XAS analysis.

Table 2

Samples prepared for X-ray absorption spectroscopy

Sample ID	Type of sample	Mo concentration	Description
15 mM $NaMoO_4$	Solution	15 mmol L^{-1}	Solution standard
SRFA, pH 4.2	Solution	2.8 mmol L^{-1}	0.36 mmol Mo g^{-1} SRFA in 0.03 mol L^{-1} $NaNO_3$.
Fh, pH 4.2	Solid	0.56 mmol g^{-1}	0.05 mmol L^{-1} Mo(VI) sorbed to 0.089 g L^{-1} Fh, in 0.01 mol L^{-1} $NaNO_3$.
Fh, pH 7.3	Solid	0.29 mmol g^{-1}	As above
Fh + P, pH 6.4	Solid	0.08 mmol g^{-1}	As above, but with 0.2 mmol L^{-1} *o*-phosphate.
$Al(OH)_3$, pH 5.3	Solid	0.64 mmol g^{-1}	0.05 mmol L^{-1} Mo(VI) sorbed to 0.078 g L^{-1} $Al(OH)_3$, in 0.01 mol L^{-1} $NaNO_3$.
$Al(OH)_3$ + P, pH 6.2	Solid	0.04 mmol g^{-1}	As above, but with 0.2 mM *o*-phosphate.
Storå Oe, pH 4.0	Solid	0.06 mmol g^{-1}	0.5 mmol L^{-1} Mo(VI) sorbed to 8.5 g L^{-1} soil in 0.01 mol L^{-1} $NaNO_3$.
Storå Bs, pH 5.1	Solid	0.002 mmol g^{-1}	0.1 mmol L^{-1} Mo(VI) sorbed to 59 g L^{-1} soil in 0.01 mol L^{-1} $NaNO_3$.

2.4. X-ray absorption spectroscopy

Molybdenum speciation in the samples was studied using both XANES (X-ray absorption near-edge structure) and EXAFS (extended X-ray absorption fine structure) spectroscopy. Before analysis, the samples were centrifuged again to remove as much water as possible, and homogenised, but care was taken not to let them dry completely.

The measurements were conducted at the wiggler beam line 4-1 at Stanford Synchrotron Radiation Lightsource (SSRL), Stanford, USA, in February 2014. The beam line operated at 3.0 GeV and with a ring current of 490-500 mA (top-up mode). The station was equipped with a Si[220] double crystal monochromator. The measurements were performed in fluorescence mode using a 13 element Ge array fluorescence detector. A Zr filter was used to reduce Fe fluorescence and scattering contributions. The Si[220] monochromator was detuned to 75 % of maximum intensity to reduce higher-order harmonics. Internal energy calibration was made with a molybdenum foil assigned to 20,000 eV (Thompson et al., 2009). Between 5 and 10 scans were collected per sample. All EXAFS spectra were then treated in the Athena software (version 0.9.021) (Ravel and Newville, 2005). Energy calibration, averaging and background removal were carried out as described by Kelly et al. (2008). The background was removed using the AUTOBAK algorithm incorporated in Athena, with a *k*-weight of 3 and with the Rbkg parameter set to 1.05 for the organic samples (SRFA and Storå Oe), and to 0.85 for all other samples.

Normalization of the XANES spectra was made with a consistent procedure in which the spectra were baseline-corrected by subtracting a linear regression through the pre-edge region (-160 to -70 eV relative to E_0) and background-corrected using a quadratic function through the post-edge region (100 to 700 eV relative to E_0), where E_0 is the first derivative maximum of the K edge of molybdenum metal, i.e. at 20,000 eV. To indicate the valence of the molybdenum in the samples, the $E_{1/2}$ (the energy position of the main edge where the

normalized intensity equals 0.5) was determined from the normalized spectra. The pre-edge peak position was determined using peak-fit analysis in Athena, where the baseline was approximated with an arc-tan lineshape.

Wavelet transform (WT) analysis of the EXAFS spectra (Funke et al. 2005) was performed to differentiate between light (e.g. C, O) and heavy (e.g. Fe) elements (back-scatterers) at 2.5-4.5 Å from molybdenum. This qualitative analysis of backscattering contributions from higher shell atoms was performed with the Morlet WT incorporated in the Igor Pro script (Chukalina, 2010) with the parameter combination $\kappa = 6$, $\sigma = 1$ and a range of $R + \Delta R$ from 2 to 4 Å (corresponding to interatomic distances of about 2.5 to 4.5 Å). The *k*-range was from 3 to 11, i.e. the same as in the EXAFS fitting procedure.

Final data treatment of the EXAFS spectra was performed with the Artemis software (version 0.9.021) (Ravel and Newville, 2005). Theoretical scattering paths were calculated with FEFF6 (Zabinsky et al. 1995). Several combinations of scattering paths were tested in the fitting procedure before deciding what paths to use; these included both single scattering and multiple scattering (MS) paths. The coordination numbers (CN) of the first-shell paths were fixed. Values of CN were chosen to give reasonable values of the Debye-Waller factor (σ^2). For the second-shell Mo···Fe, Mo···Al and Mo···C paths, we chose to fix σ^2 to a common value, 0.01, to reduce the number of adjusted parameters. In most cases, this value was close to the value obtained when letting σ^2 float, in agreement with what was found by Arai (2010). However for the MS within the molybdate tetrahedron, σ^2 was set to the same value (0.008) as for the 15 mmol L^{-1} Na_2MoO_4 solution standard. For the organic samples, the paths originally used were calculated using FEFF6 based on a bidentate molybdenum(VI) complex with bis-homocitrate (Zhou et al. 2013). The fitting procedure was performed on the Fourier transform (FT) real part between 1 and 3.5 Å using a Hanning window (dk value = 1) and optimizing over k-weights of 1, 2 and 3 (for the organic samples the FT range was adjusted to

between 1.1 and 3.5 Å). Refined models were evaluated by means of goodness-of-fit (as evidenced by the R factor in Artemis) and qualitative comparison of WT plots of the model spectra with WT plots of the EXAFS spectra. WT of the model spectra were made with the same WT-parameters and k-ranges as for measured spectra.

2.5. Surface complexation modelling: ferrihydrite

Based on the EXAFS results on the molybdenum coordination on ferrihydrite, we re-evaluated the molybdate binding data published by Gustafsson (2003) using the CD-MUSIC model (Hiemstra and van Riemsdijk, 1996). The version of the CD-MUSIC model we used in this work was the one for ferrihydrite by Tiberg et al. (2013). The model assumes a surface area of 650 m^2 g^{-1} and a point-of-zero charge at pH 8.1. Moreover the site density of singly-coordinated groups (where molybdate is allowed to sorb) is 6.25 sites nm^{-2}, while the site density of triply-coordinated groups is 1.55 sites nm^{-2} (Tiberg et al. 2013). The Stern layer capacitances are set to 1.15 F m^{-2} (inner layer) and 0.9 F m^{-2} (outer layer) in accordance with Hiemstra and van Riemsdijk (2009). New surface complexation constants for molybdate were optimised with Visual MINTEQ (Gustafsson, 2014) using the built-in PEST algorithm of Doherty (2010). PEST uses a Gauss-Marquardt-Levenberg algorithm for parameter estimation and minimizes the weighted sum of squared differences between model-generated observation values and the measured values. As input data we used the percent adsorbed molybdate from experiments detailed by Gustafsson (2003). Surface complexation constants for phosphate and electrolyte ions were those of Tiberg et al. (2013), and these are detailed in Table 3.

2.6. Organic complexation with the Stockholm Humic Model

The SHM (Stockholm Humic Model) (Gustafsson, 2001) was used to simulate the binding of molybdenum(VI) and major cations (Ca, Mg, Na, K, Al and Fe) to the Risbergshöjden Oe

and Paskalampa Oi soils. The SHM is a discrete-site / electrostatic model in which the HA or FA is assumed to have eight proton-binding sites with different acid-base characteristics. Metals/ions bind to HA or FA by forming monodentate and bidentate complexes, or by electrostatic attraction. The use of the model for soil suspensions has been detailed in other publications (Gustafsson and Kleja, 2005; Gustafsson et al. 2007; Gustafsson et al. 2011). The number of reactive sites was optimized with an acid-base batch titration method, using the assumption that 75 % of the active organic matter consisted of humic acid, while the remainder was fulvic acid (Gustafsson et al. 2007). We used the same parameters for binding of protons and major cations as earlier (Gustafsson et al. 2011; Sjöstedt et al. 2013). Equilibrium constants for the complexation of major cations are given in Table 4.

Table 3

Surface complexation reactions and constants used in the CD-MUSIC model for ferrihydrite.

Reaction	$(\Delta z_0, \Delta z_1, \Delta z_2)$[a]	log *K*	Data source(s)
$FeOH^{-½} + H^+ \leftrightarrow FeOH_2^{+½}$	(1,0,0)	8.1	[b]
$Fe_3O^{-½} + H^+ \leftrightarrow Fe_3OH^{+½}$	(1,0,0)	8.1	Assumed the same as above[b]
$FeOH^{-½} + Na^+ \leftrightarrow FeOHNa^{+½}$	(0,1,0)	-0.6	Hiemstra & van Riemsdijk (2006)
$Fe_3O^{-½} + Na^+ \leftrightarrow Fe_3ONa^{+½}$	(0,1,0)	-0.6	”
$FeOH^{-½} + H^+ + NO_3^- \leftrightarrow FeOH_2NO_3^{-½}$	(1,-1,0)	7.42	”
$Fe_3O^{-½} + H^+ + NO_3^- \leftrightarrow Fe_3OHNO_3^{-½}$	(1,-1,0)	7.42	”
$2FeOH^{-½} + 2H^+ + PO_4^{3-} \leftrightarrow Fe_2O_2PO_2^{2-} + 2H_2O$	(0.46,-1.46,0)	27.59	Tiberg et al. (2013)
$2FeOH^{-½} + 3H^+ + PO_4^{3-} \leftrightarrow Fe_2O_2POOH^- + 2H_2O$	(0.63,-0.63,0)	32.89	”
$FeOH^{-½} + 3H^+ + PO_4^{3-} \leftrightarrow FeOPO_3H_2^{-½} + H_2O$	(0.5,-0.5,0)	30.23	”
$2FeOH^{-½} + 2H^+ + MoO_4^{2-} \leftrightarrow Fe_2O_2MoO_2^- + 2H_2O$	(0.5,-0.5,0)	18.71[c]	This study
$FeOH^{-½} + H^+ + MoO_4^{2-} \leftrightarrow FeOH_2^{+½}\cdots MoO_4^{2-}$	(0.8,-1.8,0)	11.06[c]	“

[a] The change of charge in the *o*-, *b*- and *d*-planes respectively.

[b] The log *K* values of the singly- and triply-coordinated surface groups were set equal in line with Hiemstra and van Riemsdijk (1999) and the values correspond to the point-of zero charge of ferrihydrite (Dzombak and Morel, 1990).

[c] The 95 % confidence intervals, as estimated by PEST (Doherty, 2004) were (18.53, 18.88) and (10.75, 11.38) for $Fe_2O_2MoO_2^-$ and $FeOH_2^{+½}\cdots MoO_4^{2-}$, respectively.

Table 4

Complexation reactions to soil organic matter in the Stockholm Humic Model (SHM)[a]

Reaction	$(\Delta z_0, \Delta z_1)$[b]	log K	ΔLK_2
$2ROH + Al^{3+} \leftrightarrow (RO)_2Al^+ + 2H^+$	(-0.2,1.2)	-4.06	1.06
$2ROH + Al^{3+} + H_2O \leftrightarrow (RO)_2AlOH + 3H^+$	(-0.2,0.2)	-9.45	1.06
$ROH + Ca^{2+} \leftrightarrow ROCa^+ + H^+$	(-0.5,1.5)	-2.2	0.3
$ROH + Mg^{2+} \leftrightarrow ROMg^+ + H^+$	(-0.5,1.5)	-2.5	0.3
$2ROH + Fe^{3+} \leftrightarrow (RO)_2Fe^+ + 2H^+$	(-0.2,1.2)	-1.68	1.7
$2ROH + Fe^{3+} + H_2O \leftrightarrow (RO)_2FeOH + 3H^+$	(-0.2,0.2)	-4.6	1.7
$ROH + MoO_4^{2-} + H^+ + H_2O \leftrightarrow ROMoO_2(OH)_2H_2O^-$	(-0.3,-0.7)	8.6	2.5 / 1.6[c]

[a] Reactions for $Ca^{2+}$and Mg^{2+} are from Gustafsson et al. (2007), those for Fe^{3+} are from Sjöstedt et al. (2013), those for Al^{3+} are from Gustafsson et al. (2011), and the one for MoO_4^{2-} is for the Risbergshöjden Oe soil of this study.

[b] The change of charge in the *o*- and *d*-planes respectively.

[c] The ΔLK_2 value was 2.5 for solid-phase organic matter, and 1.6 for dissolved organic matter.

3. Results

3.1. Batch experiments with soils

At low pH, molybdate was adsorbed to all investigated soils, but at higher pH there was a steep adsorption edge where adsorption dropped to low values within a small pH range (Fig. 1). This is in agreement with observations for other soils (Goldberg et al. 2008). The Risbergshöjden Bs2 sample had the strongest binding, with 73% molybdenum(VI) adsorption at pH 6.9. In Fig. 1 an adsorption edge from the ferrihydrite data of Gustafsson (2003) is shown for comparison. In this case 75% molybdenum(VI) adsorption was maintained at pH 7.4. The weaker adsorption observed for Risbergshöjden Bs2 may be due to the presence of competing ions (e.g. *o*-phosphate, organic matter). The Björkby A soil was also able to bind molybdate(VI) although more weakly than the B horizons. This is probably due to the smaller amount of oxalate-extractable Fe and Al in combination with significant competition for binding sites from organic matter.

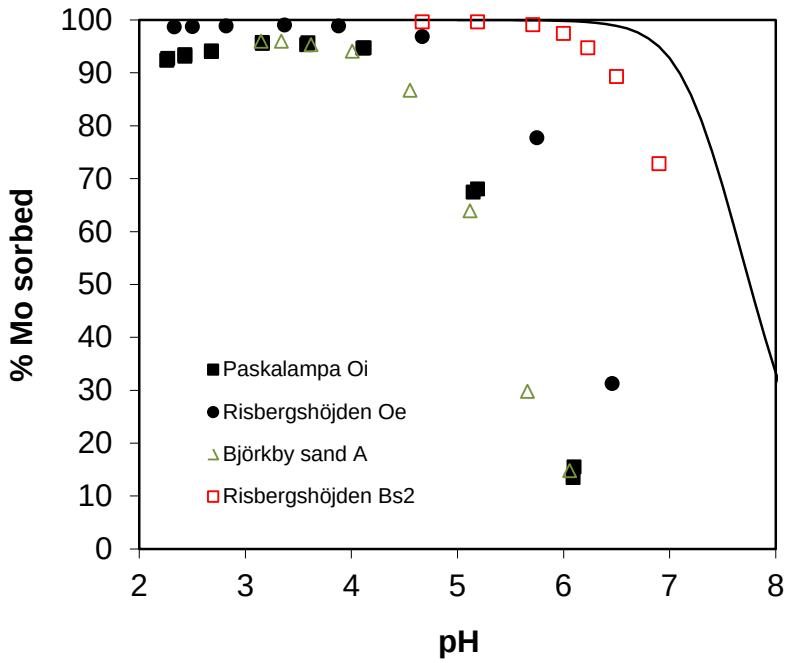

Fig. 1. Percentage sorbed molybdenum to four different soils as a function of pH in a background of 0.01 mol L^{-1} $NaNO_3$. The solid line is a model fit showing the expected Mo(VI) sorption to 3 mmol L^{-1} Fe as ferrihydrite after the addition of 50 µmol L^{-1} Mo(VI).

The organic soils also adsorbed molybdenum(VI), despite the even smaller amounts of oxalate-extractable Fe and Al in these samples (Table 1). In this case > 75% molybdenum(VI) adsorption was observed only at pH < 5. In an experiment with Paskalampa Oi, where 1.4 mmol L^{-1} *o*-phosphate was also added to the suspension, it was found that molybdenum(VI) binding was unaffected (Fig. S1, Supporting materials), while only a small percentage (~15%) of the *o*-phosphate was sorbed, independent of the pH value. The seemingly small competition effect indicated that molybdenum(VI) binding involved a mechanism that was not relevant for *o*-phosphate in this organic soil sample.

3.2. XANES spectroscopy

All XANES spectra had a pre-edge feature with centroid positions ranging from 20,002 to 20,005 eV (Fig. 2; see exact positions in Table S1, Supporting materials). Such pre-edge

features are typical for hexavalent molybdenum, especially when it occurs in tetrahedral configuration, and it is attributed to dipolar $1s \rightarrow 4d$ electronic transitions (Farges et al. 2007). The pre-edge feature was most intense for the 15 mmol L^{-1} Na_2MoO_4 sample, and less intense for $Al(OH)_3$ and Fh samples with sorbed Mo, which may result from slight distortions of the tetrahedral configuration due to binding to Fe or Al. The organic samples SRFA and Storå Oe had the least intense pre-edge features, which is consistent with Mo being in a distorted octahedral configuration in these samples (Farges et al. 2007; Arai, 2010).

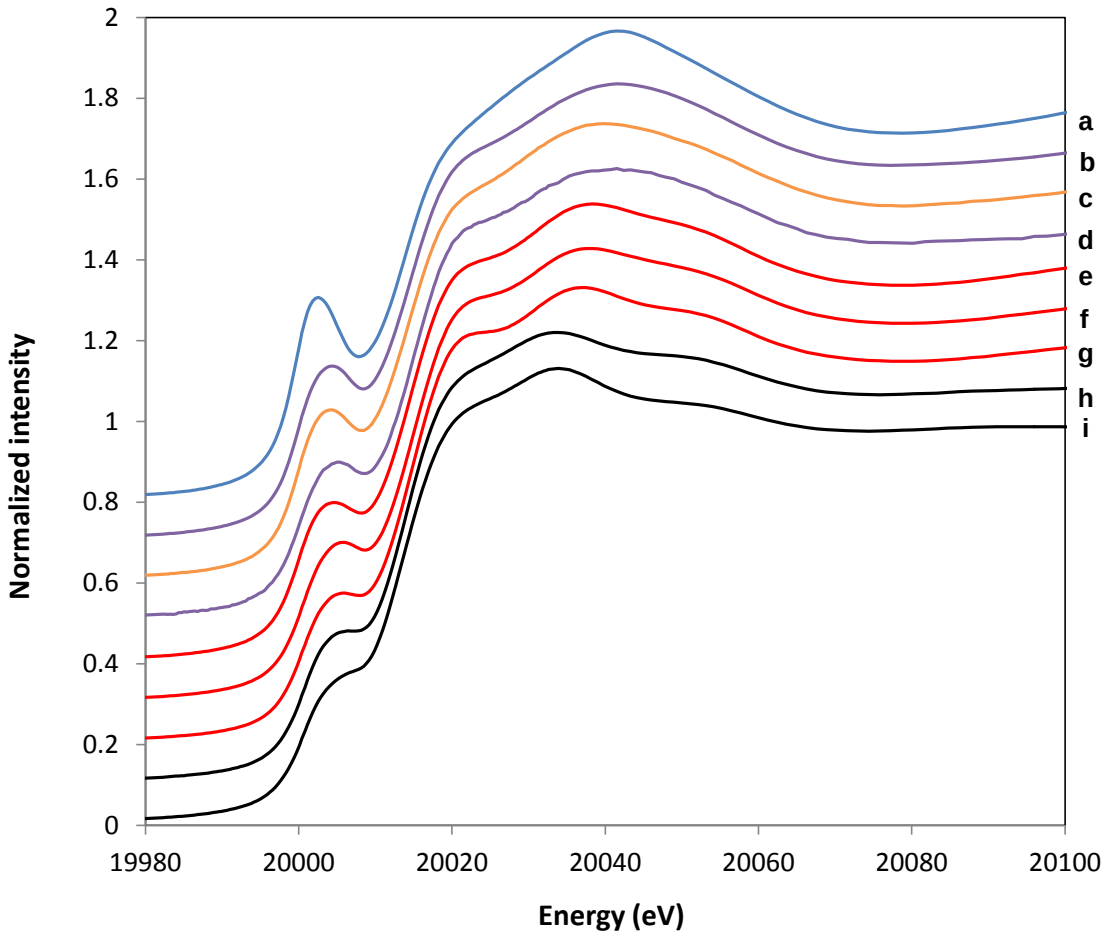

Fig. 2. Normalized, stacked Mo K-edge XANES spectra, sorted after the pre-edge intensity: a) 15 mM $NaMoO_4$, b) $Al(OH)_3$, pH 5.3, c) Storå Bs, d) $Al(OH)_3$ + P, pH 6.2, e) Fh, pH 7.3, f) Fh, pH 4.2, g) Fh + P, pH 6.3, h) SRFA, pH 4.2, i) Storå Oe, pH 4.0.

The position of the main edge was very similar for all samples, with the SRFA and Storå Oe samples having around 1 eV lower $E_{½}$ values than all the others (Table S1, Supporting materials). Again this is consistent with the former being dominated by molybdenum(VI) in a distorted octahedral configuration, whereas the other samples contained tetrahedral molybdate (Farges et al. 2007). Significant reduction of molybdenum(VI) to lower valence states should have resulted in even lower $E_{½}$ values, as well as weaker pre-edge features.

The two soil samples studied were clearly different as concerns their molybdenum speciation. As mentioned above, the Storå Oe sample was similar to the SRFA sample, and the XANES results indicated that the speciation of molybdenum was dominated by octahedrally coordinated molybdenum(VI). A closer inspection of the XANES spectrum of the Storå Bs sample revealed that it was very similar to $Al(OH)_3$ samples with sorbed Mo, but clearly different from the Fh samples with sorbed Mo (Fig. 3). Linear combination fitting (LCF) in Athena, in which Fh and $Al(OH)_3$ were assumed to be end-members, indicated that between 70 and 80 % of the molybdenum was bound to an $Al(OH)_3$-type phase rather than Fh (data not shown).

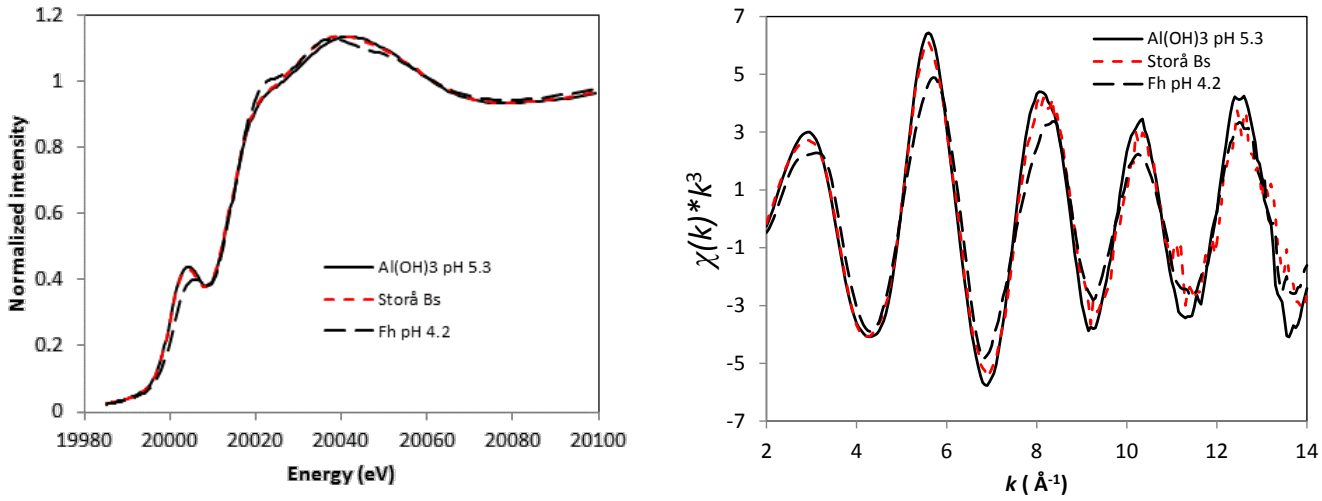

Fig. 3. The Mo K-edge XANES (left) and EXAFS spectra for the Storå Bs sample, as compared to molybdate sorbed to $Al(OH)_3$(s) at pH 5.3 and molybdate sorbed to ferrihydrite at pH 4.2.

3.3. EXAFS spectroscopy

The visual appearance of the EXAFS spectra confirmed that the two organic samples (SRFA and Storå Oe) were distinctly different from those of the other samples (Fig. 4). In the latter, the first-shell contribution was dominated by a single peak in the Fourier Transforms (FT). This could be described accurately with a model that contained tetrahedral molybdate having 4 Mo-O interatomic distances of ~1.76 Å (Table 5). This is in excellent agreement with results published earlier for similar systems (Arai, 2010; Kashiwabara et al. 2011). In the organic samples the first shell was dominated by two contributions that were identified as 2 Mo=O at 1.75 Å and 2 Mo-O at 2.00 Å. Further, in the SRFA sample a third interaction at 2.25 Å was identified. These distances are typical of a distorted octahedral configuration as found in various Mo-organic complexes (e.g. Zhou et al. 2013) as well as in molybdic acid (Liu et al. 2013). Further, they are similar to those obtained after adding molybdenum(VI) to *Brassica* seedlings (Hale et al. 2001) and to litter layer material (Wichard et al. 2009).

The second-shell contributions were different depending on the sample. For the Na_2MoO_4 solution standard, the second shell was dominated by multiple scattering (MS) within the MoO_4 tetrahedron (Mo-O-O). In the WT modulus this contribution was visible as a high-intensity area at low *k* (Fig. S2, Supporting materials). This MS contribution was assumed to be present also in the other samples where tetrahedral molybdate dominated the first shell. In addition, for all Fh samples with sorbed Mo, there was a strong contribution from Mo···Fe at ~2.80 Å. This feature, which suggests an important role of an edge-sharing bidentate complex, was also observed previously for Mo-goethite systems (Arai et al. 2010). In addition, for the Fh, pH 4.2 sample, a second Mo···Fe contribution was identified, with an interatomic distance of 3.55 Å. This suggests the additional presence of a corner-sharing bidentate complex. The fitted CN:s indicate that the edge-sharing bidentate complex may

Table 5

Fitting parameters of the EXAFS spectra for molybdenum at room temperature [a].

Sample	Path	CN	R / Å	σ^2 / Å^2	S_o^2	ΔE / eV	R
15 mM Na_2MoO_4	Mo-O	*4*	1.768(4)	0.001(1)	0.87(8)	-1.3(1.3)	0.012
pH 8.0	Mo-O-O	*3×4*	3.21(6)	0.008(11)			
Fh	Mo-O	*4*	1.754(8)	0.003(1)	0.68(6)	-3.6(1.5)	0.006
pH 4.2	Mo-O-O	*3×4*	3.38(7)	*0.008*			
	Mo⋯Fe1	0.76(26)	2.81(3)	*0.01*			
	Mo⋯Fe2	0.38(58)	3.55(10)	*0.01*			
Fh	Mo-O	*4*	1.760(6)	0.004(1)	0.77(6)	-5.9(1.1)	0.007
pH 7.3	Mo-O-O	*3×4*	3.33(4)	*0.008*			
	Mo⋯Fe1	0.84(20)	2.80(2)	*0.01*			
Fh + P	Mo-O	*4*	1.748(9)	0.004(1)	0.68(7)	-6.9(1.7)	0.014
pH 6.4	Mo-O-O	*3×4*	3.34(6)	*0.008*			
	Mo⋯Fe1	0.91(26)	2.80(3)	*0.01*			
$Al(OH)_3$	Mo-O	*4*	1.759(6)	0.002(1)	0.79(6)	-4.8(1.1)	0.007
pH 5.3	Mo-O-O	*3×4*	3.22(5)	*0.008*			
	Mo⋯Al	0.91(29)	2.62(3)	*0.01*			
$Al(OH)_3$ + P	Mo-O	*4*	1.756(7)	0.002(1)	0.71(7)	-4.3(1.3)	0.010
pH 6.2	Mo-O-O	*3×4*	3.22(6)	*0.008*			
	Mo⋯Al	1.14(32)	2.61(3)	*0.01*			
Storå Bs	Mo-O	*4*	1.750(6)	0.003(1)	0.78(7)	-5.8(1.2)	0.007
pH 5.1	Mo-O-O	*3×4*	3.18(5)	*0.008*			
	Mo⋯Al	0.50(29)	2.63(6)	*0.01*			
SRFA	Mo-O1	*2*	1.759(10)	0.001(2)	0.92(18)	10.9(1.4)	0.005
pH 4.2	Mo-O2	*2*	1.99(2)	0.003(2)			
	Mo-O3	*1*	2.25(5)	*0.01*			
	Mo⋯C1	1.86(32)	3.33(4)	*0.01*			
	Mo⋯C2	*1.86*	*3.42*	*0.01*			
Storå Oe	Mo-O1	*2*	1.735(9)	*0.001*	0.83(5)	7.4(1.7)	0.010
pH 4.0	Mo-O2	*2*	2.00(1)	0.008(2)			
	Mo⋯C1	2.07(26)	3.29(4)	*0.01*			
	Mo⋯C2	*2.07*	*3.38*	*0.01*			

[a] CN = coordination number, R = mean half-path length, σ^2 = Debye-Waller factor, S_o^2 = amplitude reduction factor, ΔE = fitted energy-shift parameter, R = goodness-of-fit parameter in Artemis. Values in italics were fixed during optimization.

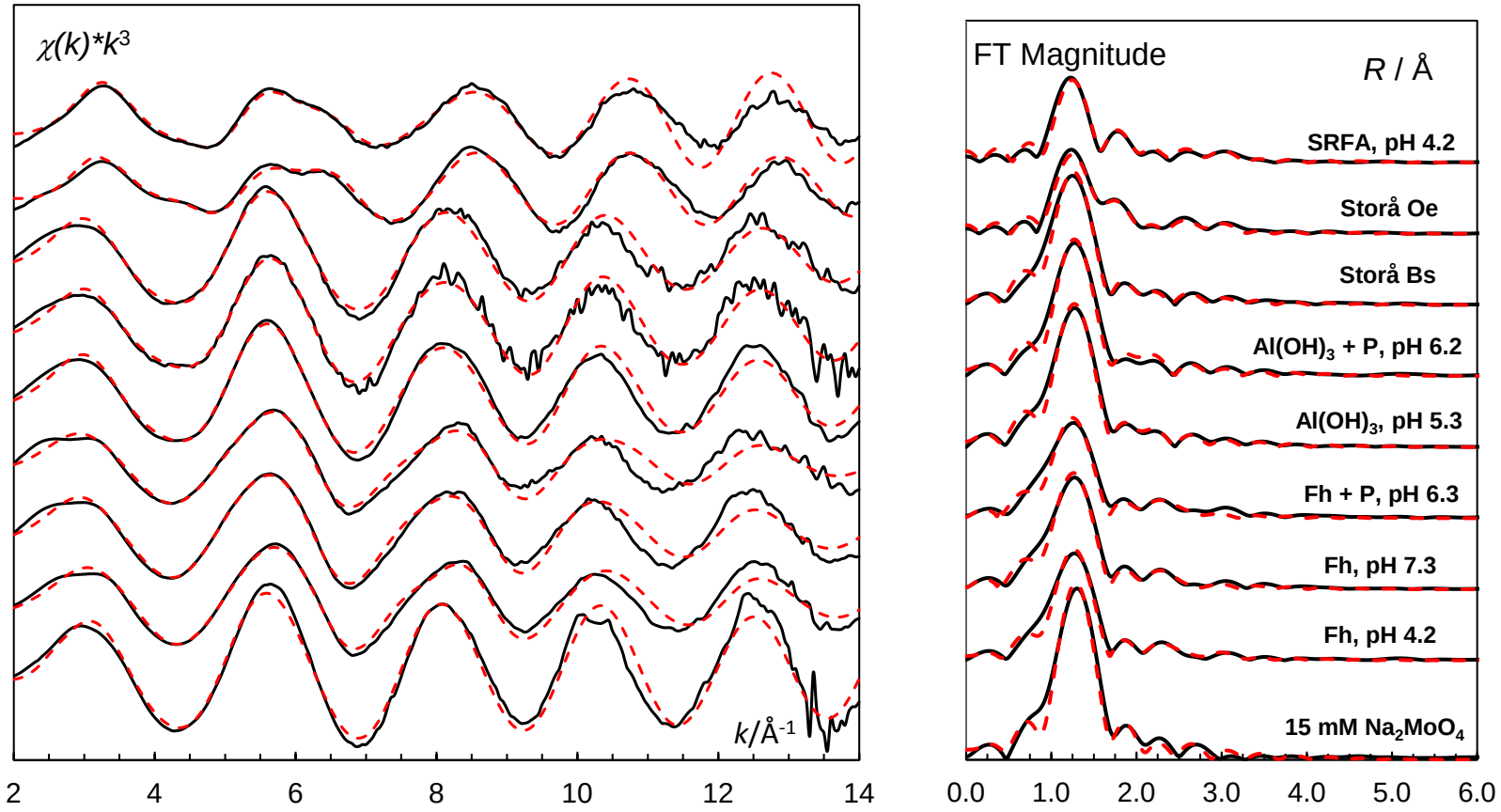

Fig. 4. Left: stacked k^3-weighted *K*-edge EXAFS spectra for molybdenum. Lines are raw data and dashed lines are best fits. Right: Fourier Transforms (FT:s) of the k^3-weighted EXAFS spectra. Lines are raw data and dashed lines are best fits.

constitute around 75 % of the bound molybdate in this sample. In the two other Fh samples, the corner-sharing bidentate complex was not identified. The second shell of the $Al(OH)_3$ samples were both dominated by Mo···Al at ~2.62 Å, which indicates a predominance of edge-sharing complexes.

For both organic samples, the second-shell contributions were found to be weak. The WT modulus suggested that the second shell was dominated by a light element (Fig. S2, Supporting materials), and it was found that a model that included a carboxylate group and an alkoxy group with Mo···C1 and Mo··· C2 distances of about 3.3 and 3.4 Å, respectively, was able to describe the data well. These distances are larger than those expected for many Mo-organic complexes, where coordination is through the Mo-O bonds (Zhou et al. 2013). We were not able to observe significant contributions from Mo···Mo distances, which were identified by Hale et al. (2001) and by Arai (2010) in some samples, or by Mo-S distances, which were found by Wichard et al. (2009).

Further, we compared the EXAFS function of Storå Bs to those Fh and $Al(OH)_3$ with sorbed molybdenum(VI) (Fig. 3). Similar to what we found for the XANES data it was revealed that the Storå Bs sample resembled Mo sorbed to $Al(OH)_3$ rather than Mo sorbed to Fh, confirming that an $Al(OH)_3$-type component accounted for most of the molybdenum(VI) binding in the Storå Bs sample. This is also clear from the model results in Table 5, according to which the second-shell contribution was dominated by edge-sharing bidentate complexes to $Al(OH)_3$.

3.4. Surface complexation model for ferrihydrite

Some earlier attempts to develop models for molybdate adsorption to ferrihydrite and goethite were built on the assumption that molybdenum(VI) forms a monodentate complex (Gustafsson, 2003; Xu et al. 2006b). However, the EXAFS data of the current study show that this is incorrect, as bidentate rather than monodentate complexes are formed. Therefore the

molybdate adsorption data of Gustafsson (2003) were re-evaluated using the CD-MUSIC model for ferrihydrite (Tiberg et al. 2013). Several different combinations of complexes were tested in the fitting. Models that contained only one or two bidentate complexes were not able to describe the whole data set, including the competition with phosphate. However, when an outer-sphere surface complex $FeOH_2^{½+}\cdots MoO_4^{2-}$ was introduced into the model, and combined with one bidentate complex, the data were described well, with reasonable confidence intervals (Table 3; Fig. 5). Such a complex was also included by Goldberg et al. (2008) when modelling molybdenum(VI) adsorption to amorphous iron and aluminium oxide using the triple layer model. An outer-sphere complex would not be readily identified by EXAFS spectroscopy. In addition, recent X-ray scattering results for the related SO_4^{2-} anion showed a significant role of such an outer-sphere complex (Zhu et al. 2014). With this combination of complexes, the model was also able to simulate the competition of molybdenum(VI) on phosphate adsorption to Fh correctly (Fig. S3, Supporting materials).

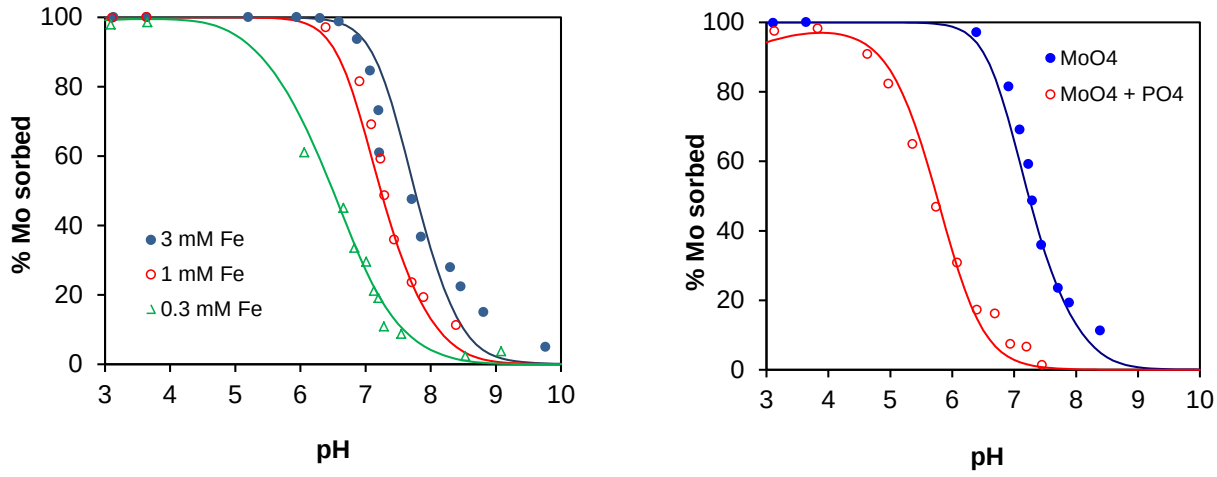

Fig. 5. Sorbed molybdenum as a function of pH in ferrihydrite suspensions in 0.01 mol L^{-1} $NaNO_3$. Left: Sorbed molybdate in systems to which 50 µmol L^{-1} Mo(VI) had been added. Right: The effect of PO_4 competition (added P = 200 µmol L^{-1}) in systems with 50 µmol L^{-1} Mo(VI) and 1 mmol L^{-1} Fe as ferrihydrite. The points are observations (data from Gustafsson, 2003), whereas the lines are model fits using the CD-MUSIC complexation constants of Table 3.

The model simulations suggest that the outer-sphere complex is important especially at high pH, and at low levels of competing anions, whereas the bidentate complex predominates under other conditions (Fig. S4, Supporting materials). When a high concentration of *o*-phosphate was introduced, the contribution from the outer-sphere complex almost vanished.

3.5. Modelling molybdenum(VI) binding to organic matter

Molybdenum(VI) binding data from Risbergshöjden Oe were used to set up a molybdenum binding reaction in SHM and to optimize its binding constant and heterogeneity (ΔLK_2) value. Data were available on the pH and concentration dependences of molybdenum(VI) binding, in two different background electrolytes (0.01 and 0.1 mol L^{-1} $NaNO_3$). It was found that a single monodentate complex with the composition $ROMoO_2(OH)_2H_2O^-$ was sufficient to describe the binding data very well (Fig. 6). This complex can be thought of as molybdic acid bound to a carboyxlic acid group of natural organic matter through one of the distant Mo-O bonds, whereas the oxygens at intermediate distances (Mo-O = 2.00 Å) are both protonated, in line with what would be expected for molybdic acid (Liu et al. 2013). This interpretation agrees very well with the EXAFS data. This complex was able to account for the observed difference between 0.01 and 0.1 mol L^{-1} background electrolytes (Fig. 6). However, for optimal fit the ΔLK_2 value needed to be different for dissolved and for solid-phase organic matter in the Risbergshöjden Oe suspensions, i.e. 1.6 and 2.5, respectively (Table 4).

Although there was only one observation on molybdenum(VI) binding for the Storå Oe soil, this was consistent with the model calibrated for the Risbergshöjden Oe soil (Fig. 6). By contrast, the model was not able to describe molybdenum(VI) binding to Paskalampa Oi, in which molybdenum(VI) binding was weaker (Fig. 6). When the log *K* value of the $ROMoO_2(OH)_2H_2O^-$ complex was decreased by nearly an order of magnitude, from 8.6 to 7.7 (dashed line in Fig. 6), the model was finally able to simulate the data well.

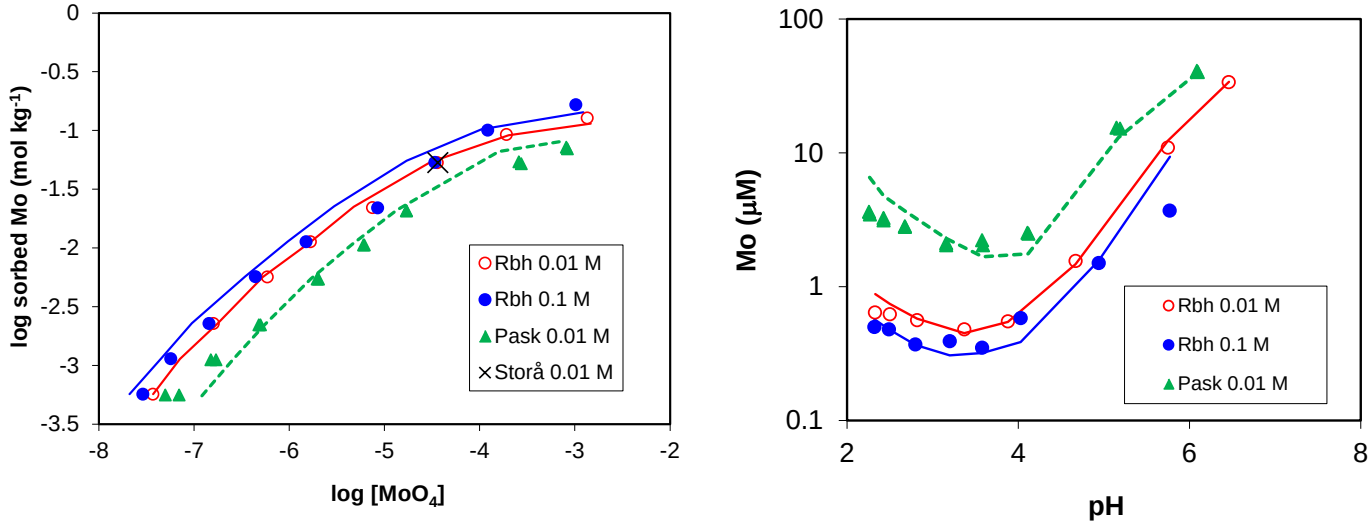

Fig. 6. Molybdenum sorption to the O horizons after 8 d. a) Sorbed molybdenum as a function of dissolved molybdenum; b) Dissolved molybdenum as a function of pH after the addition of 50 µmol L^{-1} Mo, equivalent to ~6 mmol kg^{-1}, The points are observations, whereas solid lines are model fits with the SHM using complexation constants shown in Table 4. For the Paskalampa Oi horizon, the dashed line represents the model fit with log *K* of the Mo-organic complex set to 7.7 instead of 8.6.

4. Discussion

Molybdate can coordinate with both iron and aluminium (hydr)oxides and with organic matter, all of which are very common in soils. This may be ecologically important in acid, nutrient-poor soils, as these processes act to prevent leaching of this trace element and thus keep it bioavailable.

The former process, i.e. binding to iron and aluminum (hydr)oxides, is the best known of the two. Our results for ferrihydrite are also largely consistent with the results previously obtained for goethite (Arai, 2010). Both studies show that a mix of edge-sharing and corner-sharing bidentate complexes is formed. However, for goethite around 70% of the bound molybdate was present as corner-sharing bidentate complexes (Arai, 2010), whereas for ferrihydrite in the present study the corresponding figure was 25% or less. This difference is in line with what was found earlier for lead(II) and copper(II) (Tiberg et al. 2013), and can be

attributed to the more disordered structure of ferrihydrite, which increases the likelihood of edge-sharing coordination. The binding mode on amorphous $Al(OH)_3$ appears to be similar, with a predominance of edge-sharing complexes. This contrasts with the FTIR evidence of molybdenum(VI) coordination on gibbsite, which suggest that corner-sharing bidentate complexes predominate (Miedaner et al. 2011). Again, this difference may be related to differences in surface structure between crystalline gibbsite and the amorphous $Al(OH)_3$ used in the present investigation.

In his goethite systems, Arai (2010) found evidence for Mo···Mo interactions and possible octahedral configuration of Mo in the systems at pH values between 3 and 4. Such observations were not made in the current study, possibly because our systems were more dilute, with dissolved Mo at equilibrium below 1 μmol L^{-1} at pH < 5.

The results for the Storå Bs sample, showing a predominance of $Al(OH)_3$-bound Mo, suggest that the environmental importance of $Al(OH)_3$ or of $Al(OH)_3$-type surfaces for molybdenum(VI) may be larger than often considered. In the case of Storå Bs, the results can be at least partly explained by the much larger concentrations of oxalate-extractable Al in relation to Fe (Table 1). It should also be mentioned that the oxalate-extractable Al in Storå Bs is probably dominated by allophane and imogolite rather than by $Al(OH)_3$, in line with the findings from other Scandinavian Spodosols (Karltun et al. 2000). Likely, the $Al(OH)_3$-type phase in Storå Bs as implied by the EXAFS results is in fact allophane; further evidence for this comes from the large value of oxalate-extractable Si (Table 1). In other words, the results suggest a significant role of allophane and possibly other $Al(OH)_3$-type phases for the retention of molybdate in soils.

The modelling results suggest that outer-sphere complexes are important for molybdenum(VI) binding to ferrihydrite under certain conditions, e.g. high pH, low surface coverage and low levels of competing ions. By using a combination of an inner-sphere

bidentate complex and an outer-sphere complex, the CD-MUSIC model was able to provide a consistent description of molybdenum(VI) binding to ferrihydrite under all investigated conditions. Similarly, outer-sphere complexes are probably also important on amorphous $Al(OH)_3$ at high pH (Goldberg et al. 2008).

As observed in previous studies (Bibak and Borggaard, 1994; Wichard et al. 2009), molybdenum(VI) was bound to natural organic matter at low pH. The XANES results ruled out significant reduction of molybdenum(VI) to lower valence states, and the EXAFS data in combination with geochemical modelling suggest the formation of a weak Mo-carboxylate complex, in which molybdenum(VI) occurs in a distorted octahedral configuration similar to that of molybdic acid, and is bound to a carboxylate group through a distant oxygen of the molybdenum(VI) octahedron. This interpretation differs from that of Hale et al. (2001), as they observed strong Mo···Mo interactions in their EXAFS spectra of Mo-treated *Brassica* seedlings, suggesting the existence of polymolybdate clusters. It should be noted, however, that *Brassica* seedlings are quite different from the humic organic matter that was investigated in this study, and therefore the Mo coordination environment may not be comparable. Moreover, the relatively high concentrations of molybdenum(VI) added in their experiments (30 or 60 mg L^{-1}) is part of the explanation. For example, at equilibrium around 2.8 mg L^{-1} Mo was dissolved in the Storå Oe suspension, most of which was likely organically bound. Hence Mo polymers may not have been thermodynamically favoured in our systems. Our EXAFS results are, however, reasonably similar to those obtained by Wichard et al. (2009), although we were not able to include any Mo-S interactions in our EXAFS model. This may be related to the rather high molybdenum(VI) load (i.e. 0.06 mmol g^{-1}, see Table 2) that we used in our experiments with Storå Oe to get good EXAFS data. The total amount of reactive thiol groups in similar organic samples is expected to be in the order of 0.025 mmol g^{-1} (Skyllberg and Drott, 2010), and therefore it seems possible that all available S-containing

groups were completely saturated and that their contribution was hidden by the more numerous carboxylate groups. The large heterogeneity value (ΔLK_2) of the SHM provides further evidence for the involvement of other, stronger, ligands (such as thiols) at lower surface coverage, i.e. under environmentally realistic conditions.

We observed a difference in reactivity between the O horizons concerning their molybdenum(VI) binding: the *Sphagnum* peat sample from Paskalampa sorbed molybdenum(VI) less strongly than the Spodosol Oe horizon samples (Risbergshöjden Oe and Storå Oe). This may reflect a difference in composition of the organic ligands responsible for molybdenum(VI) binding, but more research is required to understand this.

Collectively, our and other results show that molybdenum(VI) will form a complex with natural organic matter at low pH (below about 5-6); this likely constitutes an important sorption mechanism of molybdenum(VI) in acid organic soils. The trapped molybdenum(VI) may then be taken up and converted to e.g. the iron-molybdenum cofactor of nitrogenase, in which molybdenum is coordinated in a different way (Burgess et al. 1990). Although there are limitations with the EXAFS method as discussed above, our work confirms that molybdenum(VI) sorption to organic matter is important, and that it involves complexes with monomeric molybdenum(VI) in a distorted octahedral configuration.

5. Conclusions

Molybdenum(VI) is able to bind to iron(III), aluminium(III) and organic matter, all common constituents of soils. More specifically we found that:

- According to EXAFS spectroscopy, molybdenum(VI) coordinates to ferrihydrite primarily as an edge-sharing bidentate complex involving tetrahedral molybdate, with minor contributions of a corner-sharing bidentate complex. In addition, geochemical

modelling implies the existence of an outer-sphere surface complex, which is of some importance at high pH.

- On amorphous $Al(OH)_3$, molybdenum(VI) forms edge-sharing bidentate complexes similar to those on ferrihydrite. The binding of molybdenum(VI) to a spodic Bs horizon was similar to that of amorphous $Al(OH)_3$, indicating a preference for binding onto $Al(OH)_3$-type phases such as allophane.
- On natural organic matter, which were represented by Suwannee River Fulvic Acid and a mor layer from a Spodosol, added molybdenum(VI) was recovered as a distorted octahedral monomeric complex, which was stable at low pH. The Stockholm Humic Model was able to describe this interaction well assuming monodentate coordination between a distant oxygen of the molybdenum(VI) octahedron and a carboxylate group. Phosphate did not compete significantly with molybdate for sorption sites.
- These results show that acid, nutrient-poor ecosystems (e.g., peat soils and Spodosols) contain sorbents able to trap molybdenum efficiently, thus preventing the loss of this important trace element to waters.

Acknowledgements

This study was partly funded by a grant from the Geological Survey of Sweden. Portions of this research were carried out at the Stanford Synchrotron Radiation Lightsource, SLAC National Accelerator Laboratory, supported by the U.S. Department of Energy, Office of Science, Office of Basic Energy Sciences under Contract No. DE-AC02-76SF00515. The SSRL Structural Molecular Biology Program is supported by the DOE Office of Biological and Environmental Research, and by the National Institutes of Health, National Institute of General Medical Sciences (including P41GM103393). The contents of this publication are

solely the responsibility of the authors and do not necessarily represent the official views of NIGMS or NIH. Ingmar Persson is acknowledged for coordinating the beamtime at SSRL.

References

Arai, Y. 2010. X-ray absorption spectroscopic investigation of molybdenum multinuclear sorption mechanism on the goethite-water interface. Environ. Sci. Technol. 44, 8491-8496.

Bibak, A., Borggaard, O.K. 1994. Molybdenum adsorption by aluminum and iron oxides and humic acid. Soil Sci. 158, 323-328.

Bourikas, K., Hiemstra, T., van Riemsdijk, W.H. 2001. Adsorption of molybdate monomers and polymers on titania with a multisite approach. J. Phys. Chem. B 105, 2393-2403.

Burgess, B.K. 1990. The iron-molybdenum cofactor of nitrogenase. Chem. Rev. 90, 1377-1406.

Chukalina, M. 2010. Wavelet2.ipf, a procedure for calculating the Wavelet transform in IGOR Pro. Downloaded from website in November 2011: http://www.esrf.eu/UsersAndScience/Experiments/CRG/BM20/Software/Wavelets/IGOR

Doherty, J. 2010. PEST – Model-independent parameter estimation. User manual, 5th edition. Watermark Numerical Computing, Web: http://www.pesthomepage.org.

Dzombak, D.A., Morel, F.M.M. 1990. Surface complexation modeling. Wiley & Sons, New York.

Farges, F., Siewert, R., Brown, G.E., Guesdon, A., Morin, G. 2006. Structural environments around molybdenum in silicate glasses and melts. I. Influence of composition and oxygen fugacity on the local structure of molybdenum. Can. Mineral. 44, 731-753.

Funke H., Scheinost A.C. and Chukalina M. 2005. Wavelet analysis of extended x-ray absorption fine structure data. Phys. Rev. B 71, 094110.

Goldberg, S., Forster, H.S., Godfrey, C.L. 1996. Molybdenum adsorption on oxides, clay minerals, and soils. Soil Sci. Soc. Am. J. 60, 425-432.

Goldberg, S., Johnston, C.T., Suarez, D.L., Lesch, S.L. 2008. Mechanism of molybdenum adsorption on soils and soil minerals evaluated using vibrational spectroscopy and surface complexation modeling. In: Developments in Earth and Environmental Sciences 7 (eds. M.O. Barnett and D.G. Kent), pp. 235-266. Elsevier, Amsterdam.

Gustafsson, J.P., Bhattacharya, P., Bain, D.C., Fraser, A.R., McHardy, W.J. 1995. Podzolisation mechanisms and the synthesis of imogolite in northern Scandinavia. Geoderma 66, 167-184.

Gustafsson, J.P., Bhattacharya, P., Karltun, E. 1999. Mineralogy of poorly crystalline aluminium phases in the B horizon of Podzols in southern Sweden. Appl. Geochem. 14, 707-718.

Gustafsson, J.P. 2001. Modeling the acid-base properties and metal complexation with the Stockholm Humic Model. J. Colloid Interface Sci. 244, 102-112.

Gustafsson, J.P. 2003. Modelling molybdate and tungstate adsorption to ferrihydrite. Chem. Geol. 200, 105-115.

Gustafsson, J.P. 2014. Visual MINTEQ, version 3.1. Web: http://vminteq.lwr.kth.se.

Gustafsson, J.P., Kleja, D.B. 2005. Modeling salt-dependent proton binding by organic soils with the NICA-Donnan and Stockholm Humic models. Environ. Sci. Technol. 39, 5372-5377.

Gustafsson, J. P., Persson I., Kleja D. B., van Schaik J. W. J. 2007. Binding of iron(III) to organic soils: EXAFS spectroscopy and chemical equilibrium modeling. Environ. Sci. Technol. 41, 1232-1237.

Gustafsson, J.P., Tiberg, C., Edkymish, A., Kleja, D.B. 2011. Modelling lead(II) sorption to ferrihydrite and soil organic matter. Environ. Chem. 8, 485-492.

Hale, K.L., McGrath, S.P., Lombi, E., Stack, S.M., Terry, N., Pickering, I.J., George, G.N., Pilon-Smits, E.A.H. 2001. Molybdenum sequestration in Brassia species. A role for anthocyanins? Plant Physiol. 126, 1391-1402.

Hiemstra, T., van Riemsdijk, W.H. 1996. A surface structural approach to ion adsorption: The charge distribution (CD) model. J. Colloid Interface Sci. 179, 488-508.

Hiemstra, T., van Riemsdijk, W.H. 2006. On the relationship between charge distribution, surface hydration, and the structure of the interface of metal hydroxides. J. Colloid Interface Sci. 301, 1-18.

Hiemstra, T., van Riemsdijk, W.H. 2009. A surface structural model for ferrihydrite. I. Sites related to primary charge, molar mass and mass density. Geochim. Cosmochim. Acta 73, 4423-4436.

ISO (International Orgznization for Standardization) 2007. ISO TS 21268:2. Soil Quality – Leaching procedures for subsequent chemical and ecotoxicological testing of soil and soil materials – Part 2: Batch test using a liquid to solid ratio of 10 l/kg dry matter.

IUSS Working Group WRB 2014. World Reference Base for Soil Resources 2014. International soil classification system for naming soils and creating legends for soil maps. World Soil Resources Reports No. 106. FAO, Rome.

Jones, L.H.P. 1957. The solubility of molybdenum in simplified systems and aquoeus soil suspensions. J. Soil Sci. 8, 313-327.

Karltun, E., Bain, D.C., Gustafsson, J.P., Mannerkoski, H., Murad, E., Wagner, U., Fraser, A.R., McHardy, W.J., Starr, M. 2000. Surface reactivity of poorly-ordered minerals in podzol B horizons. Geoderma 94, 265-288.

Kashiwabara, T., Takahashi, Y., Tanimizu, M. and Usui, A. 2011. Molecular-scale mechanisms of distribution and isotopic fractionation of molybdenum between seawater and ferromanganese oxides. Geochim. Cosmochim. Acta 75, 5762-5784.

Kelly, S., Hesterberg, D., Ravel, B. 2008. Analysis of soils and minerals using X-ray absorption spectroscopy. In: *Methods of soil analysis. Part 5. Mineralogical methods.* (eds. A.L. Ulery and L.R. Drees). SSSA Book Series Ser. 5, SSSA, Madison, WI.

Kleja, D.B., Standring, W., Oughton, D.H., Gustafsson, J.P., Fifield, K., Fraser, A.R. 2005. Assessment of isotopically exchangeable Al in soil materials using ^{26}Al tracer. Geochim. Cosmochim. Acta 69, 5263-5277.

Liu, X., Cheng, J., Sprik, M., Lu, X. 2013. Solution structures and acidity constants of molybdic acid. J. Phys. Chem. Lett. 4, 2926-2930.

Manning, B.A., Goldberg, S. 1996. Modeling competitive adsorption of arsenate with phosphate and molybdate on oxide minerals. Soil Sci. Soc. Am. J. 60, 121-131.

Meima, J.A., van der Weijden, R.D., Eighmy, T.T., Comans, R.N.J. 1999. Carbonation processes in municipal solid waste incinerator bottom ash and their effect on the leaching of copper and molybdenum. Appl. Geochem. 16, 1503-1513.

Murphy, L.S., Walsh, L.M. 1972. Correction of micronutrient deficiencies with fertilizers. In: J.J. Mortvedt, P.M. Giordano, W.L. Lindsay (Eds) Micronutrients in agriculture. Soil Science Society of America, Madison, WI, pp. 347-387.

Miedaner, M.M., Weerasooriya, R., Tobschall, H.J. 2011. Molybdate interactions with gibbsite surfaces examined by macroscopic and cluster modeling. J. Geol. Soc. Sri Lanka 14, 11-19.

Ravel, B. and Newville, M. 2005. Athena Artemis Haephestus: Data analysis for X-ray absorption spectroscopy using IFEFFIT. J. Synchrotron Rad. 12, 537-541.

Reisenauer, H.M., Tabikh, A.A., Stout, P.R. 1962. Molybdenum reactions with soils and the hydrous oxides of iron, aluminum, and titanium. Soil Sci. Soc. Am. J. 26, 23-37.

Siebert, C., Pett-Ridge, J.C., Opfergelt, S., Guicharnaud, R.A., Halliday, A.N., Burton, K.W. 2015. Molybdenum isotope fractionation in soils: Influence of redox conditions, organic matter, and atmospheric inputs. Geochim. Cosmochim. Acta 162, 1-34.

Sjöstedt, C., Persson, I., Hesterberg, D., Kleja, D.B., Borg, H., Gustafsson, J.P. 2013. Iron speciation in soft-water lakes and soils as determined by EXAFS spectroscopy and geochemical modeling. Geochim. Cosmochim. Acta 105, 172-186.

Skyllberg, U., Drott, A. 2010. Competition between disordered iron sulfide and natural organic matter associated thiols for mercury(II) – an EXAFS study. Environ. Sci. Technol. 44, 1254-1259.

Spanos, N., Vordonis, L., Kordulis, C., Lycourghiotis, A. 1990. Molybdenum-oxi species deposited on alumina by adsorption. I. Mechanism of the adsorption. J. Catal. 124, 301-314.

Suttle, N.F. 1991. The interactions between copper, molybdenum and sulphur in ruminant nutrition. Annu. Rev. Nutr. 11, 121-140.

Szilagyi, M. 1967. Sorption of molybdenum by humic preparations. Geochem. Int. 4, 1165-1167.

Thompson, A., Attwood, D., Gullikson, E., Howells, M., Kim, K.-J., Kirz, J., Kortright, J., Lindau, I., Pianetta, P., Robinson, A., Scofield, J., Underwood, J., Williams, G. and Winck, H. 2009. *X-ray Data Booklet.* Lawrence Berkeley National Laboratory, University of California, Berkeley, California.

Tiberg, C., Sjöstedt, C., Persson, I., Gustafsson, J.P. 2013. Phosphate effects on copper(II) and lead(II) sorption to ferrihydrite. Geochim. Cosmochim. Acta 120**,** 140-157.

van Reeuwijk, L.P. 1995. Procedures for Soil Analysis. 5 ed.; International Soil Reference and Information Centre: Wageningen, Netherlands.

Wichard, T., Mishra, B., Myneni, S.C.B., Bellenger, J.-P., Kraepiel, A.M.L. 2009. Storage and bioavailability of molybdenum in soils increased by organic matter complexation. Nature Geosci. 2, 625-629.

Wurzberger, N., Bellenger, J.P., Kraepiel, A.M.L., Hedin, L.O. 2012. Molybdenum and phosphorus interact to constrain asymbiotic nitrogen fixation in tropical forests. PLoS One 7(3), e33710.

Xu, N., Christodoulatos, C., Braida, W. 2006a. Adsorption of molybdate and tetrathiomolybdate on pyrite and goethite: effect of pH and competitive anions. Chemosphere 62, 1726-1735.

Xu, N., Christodoulatos, C., Braida, W. 2006b. Modeling the competitive effect of phosphate, sulfate, silicate and tungstate on the sorption of molybdate onto goethite. Chemosphere 64, 1325-1333.

Zabinsky, S. I., Rehr, J. J., Ankudinov, A., Albers, R. C., Eller, M. J. 1995. Multiple-scattering calculations of X-ray-absorption spectra. Phys. Rev. B 52(4), 2995-3009.

Zhou, Z.H., Wang, H., Yu, P., Olmstead, M.M., Cramer, S.P. 2013. Structure and spectroscopy of a bidentate *bis*-homocitrate dioxo-molybdenum(VI) complex: Insights relevant to the structure and properties of the FeMo-cofactor in nitrogenase. J. Inorg Biochem. 118, 100-106.

Zhu, M., Northrup, P., Shi, C., Billinge, S.J.L., Sparks, D.L., Waychunas, G.A. 2014. Structure of sulfate adsorption complexes on ferrihydrite. Environ. Sci. Technol. Lett. 1, 97-101.

Graphical abstract:

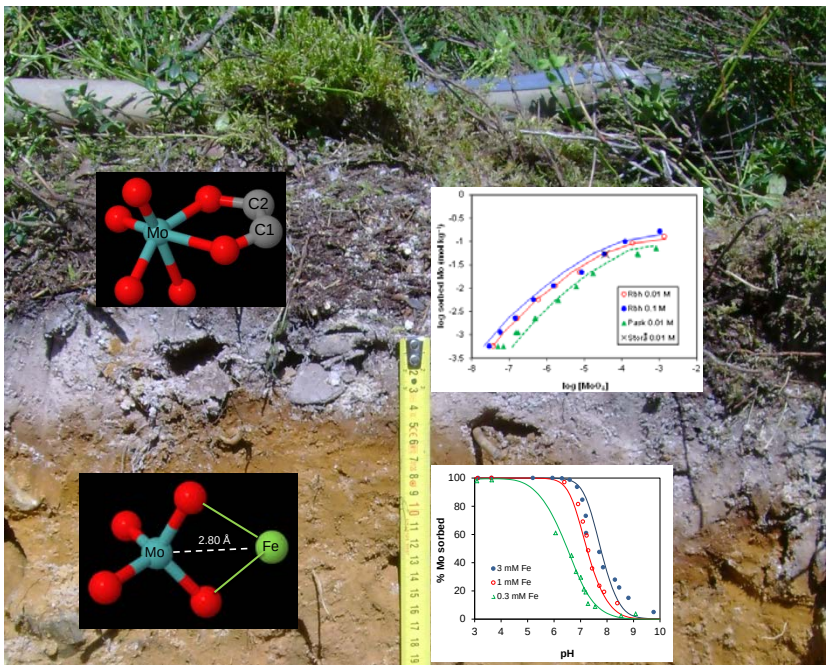

Supporting Materials

Molybdenum binding to soil constituents in acid soils: an XAS and modelling study

Jon Petter Gustafsson[a,b,*] and Charlotta Tiberg[a]

[a]*Department of Soil and Environment, Swedish University of Agricultural Sciences, Box 7014, 750 07 Uppsala, Sweden*
[b]*Division of Land and Water Resources Engineering, KTH Royal Institute of Technology, Brinellvägen 28, 100 44 Stockholm, Sweden*

*Corresponding author. E-mail address: jon-petter.gustafsson@slu.se

Content

Table S1

Pre-edge and edge positions (eV) of the Mo K-edge XANES spectra

Sample	Pre-edge position /eV[a]	$E_{½}$ / eV[b]
15 mM Na_2MoO_4	20002.4	20012.2
Fh, pH 4.2	20004.5	20012.5
Fh, pH 7.3	20003.6	20012.2
Fh + P, pH 6.4	20004.3	20012.2
$Al(OH)_3$, pH 5.3	20003.6	20012.2
$Al(OH)_3$+ P, pH 6.2	20004.1	20012.5
Storå Bs, pH 5.1	20003.4	20012.1
SRFA, pH 4.0	20004.6	20011.6
Storå Oe, pH 4.2	20004.6	20011.2

[a]The centroid position of the pre-edge, obtained using an arc-tan lineshape (as the baseline) and Gaussian functions

[b]Main edge energy at 50 % normalized absorbance

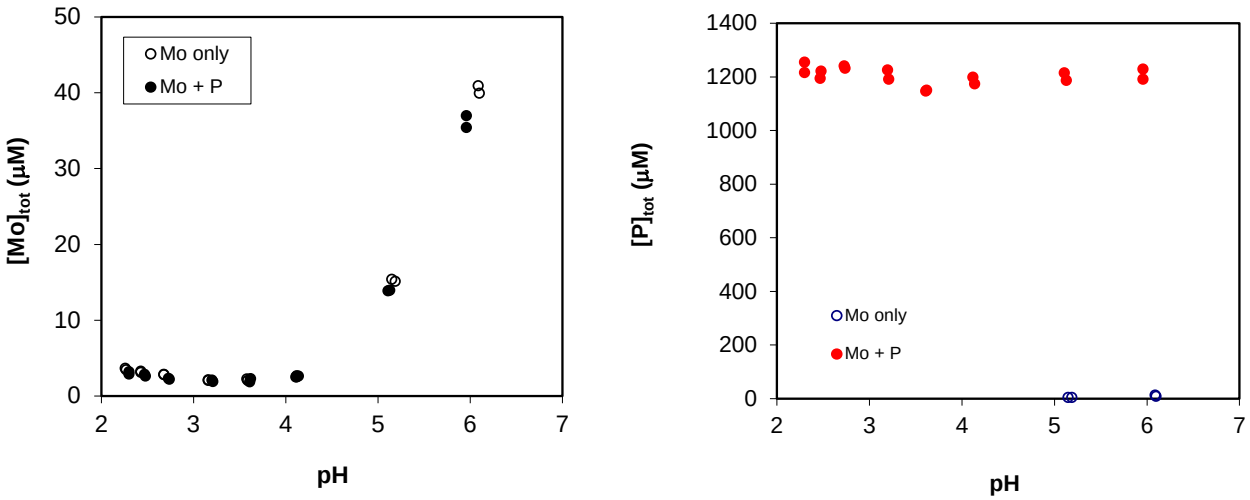

Fig. S1. Dissolved concentrations of molybdenum and phosphorus in Paskalampa Oi suspensions to which different concentrations of molybdenum and phosphorus had been added: "Mo only" initially contained 50 µmol L^{-1} molybdate(VI) and "Mo + P" contained 50 µmol L^{-1} molybdate(VI) + 1.4 mmol L^{-1} phosphate..

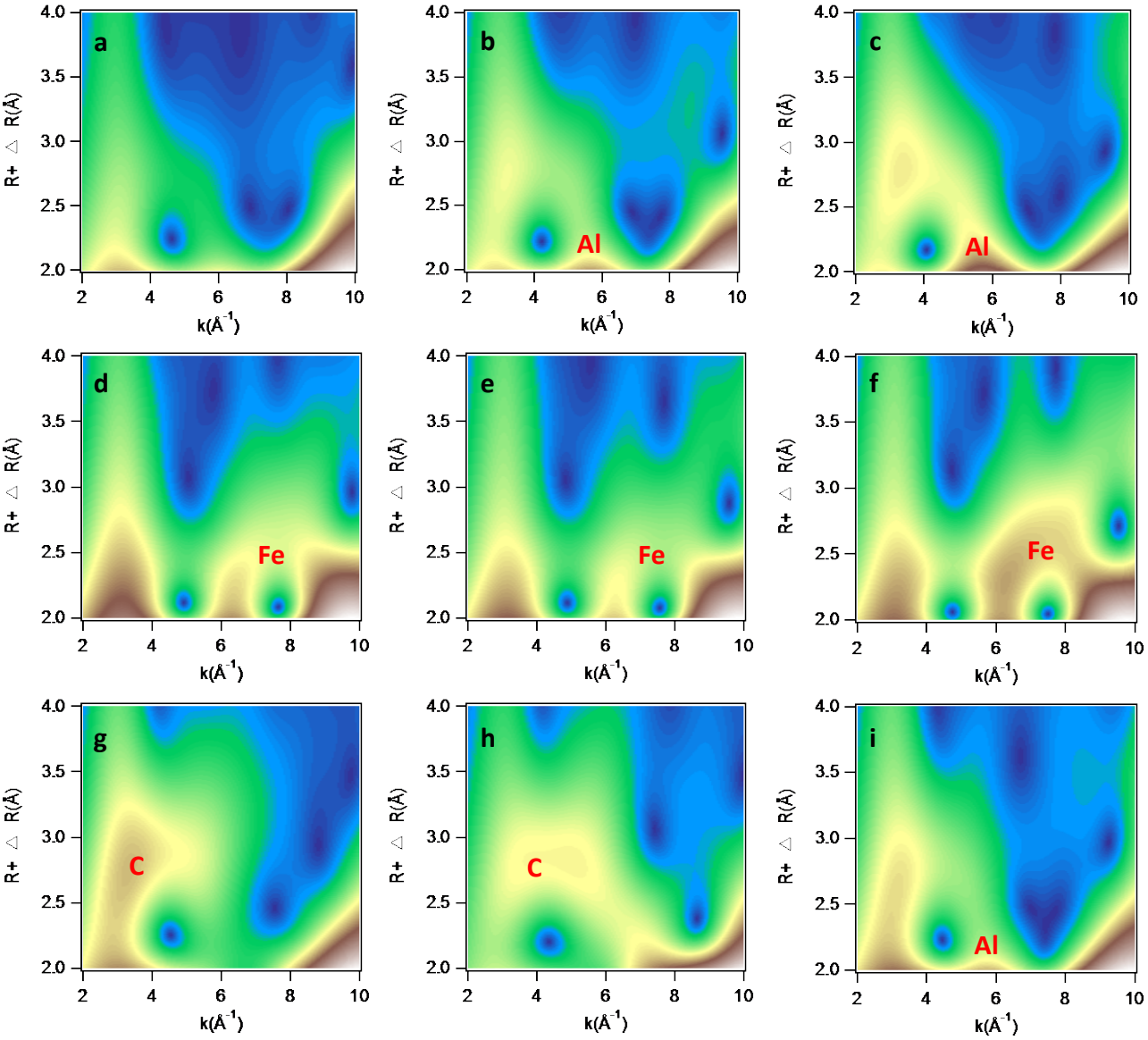

Fig. S2. High resolution Morlet WT modulus displaying the second coordination shell (κ = 6, σ = 1, *k*-range 3-11 Å^{-1}) for a) 15 mM $NaMoO_4$, b) $Al(OH)_3$, pH 5.3, c) $Al(OH)_3$ + P, pH 6.2, d) Fh, pH 4.2, e) Fh, pH 7.3, f) Fh + P, pH 6.4, g) SRFA, pH 4.0, h) Storå Oe, pH 4.2, i) Storå Bs, pH 5.1. White/brown areas indicate high intensity whereas blue/green areas indicate low intensity of the WT modulus. Second-shell contributions with elevated intensity (other than multiple scattering) are marked in red. .

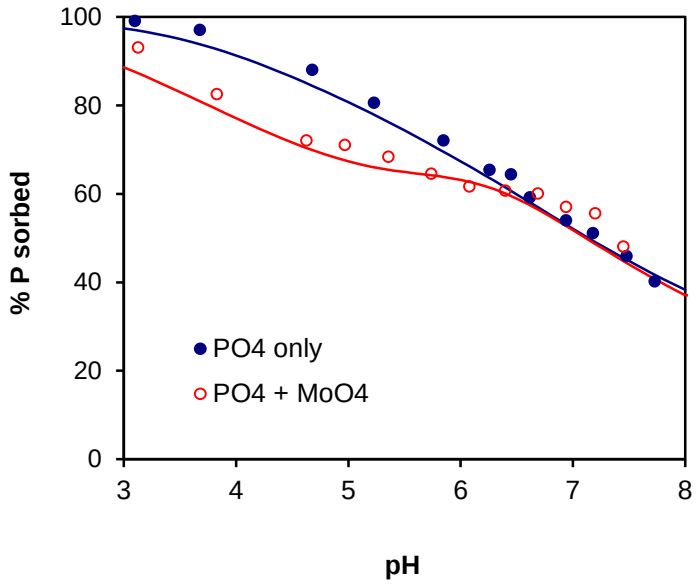

Fig. S3. Observed *o*-phosphate adsorption to ferrihydrite (P = 200 µmol L^{-1}, Fe = 1 mmol L^{-1}) in the absence or presence of added molybdenum(VI) (Mo = 50 µmol L^{-1}). Lines are model fits with the surface complexation constants of Table 3. The data are from Gustafsson (2003).

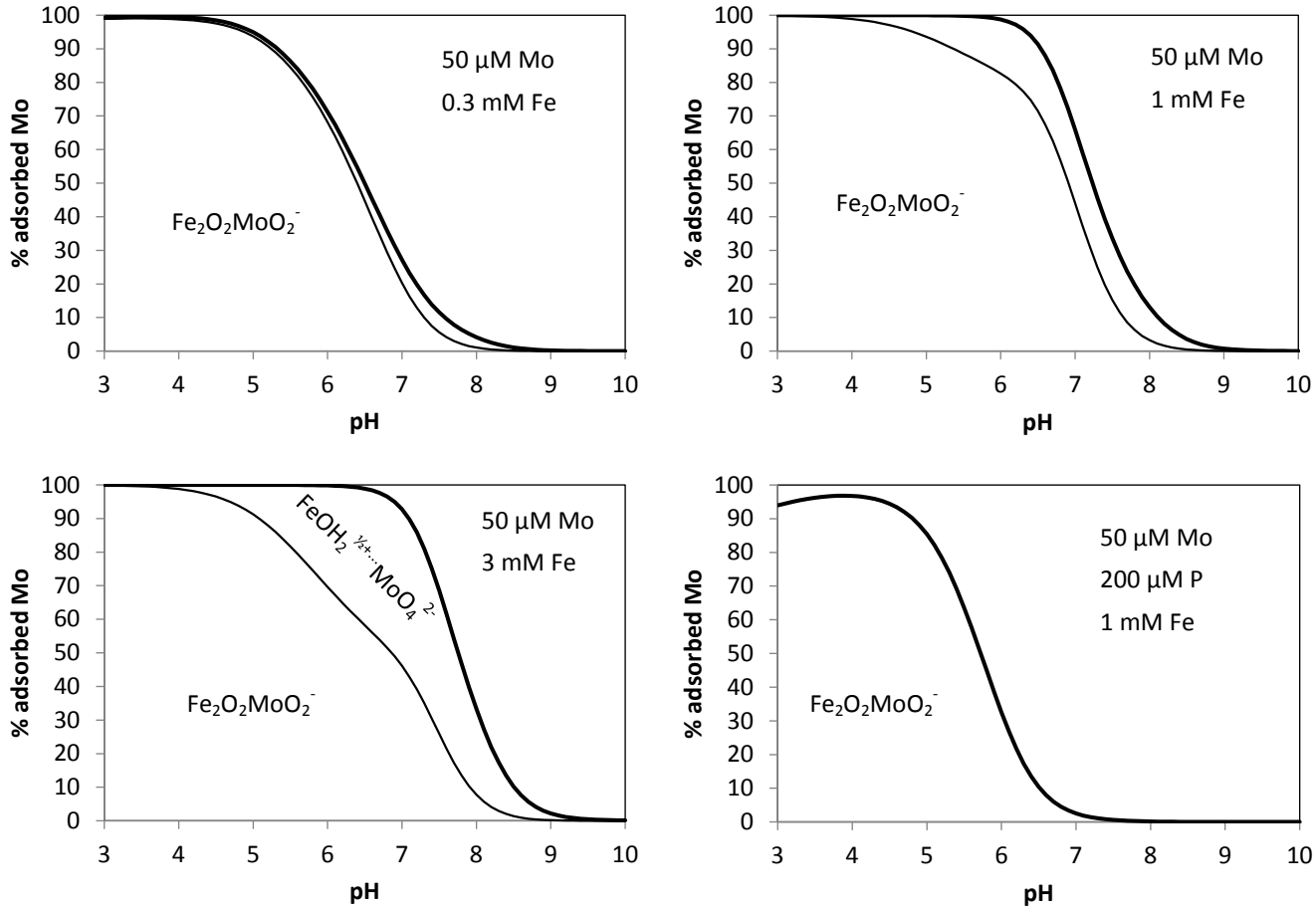

Fig. S4. Relative contributions of different molybdenum(VI) surface complexes to the simulated adsorption edges in systems with ferrihydrite. The initial composition of each system is shown in the upper right of each figure. All systems contained 0.01 mol L^{-1} $NaNO_3$.